



ELSEVIER

Computational Statistics & Data Analysis 41 (2002) 311–328

COMPUTATIONAL
STATISTICS
& DATA ANALYSIS

www.elsevier.com/locate/csda

Space–time variograms and a functional form for total air pollution measurements

S. De Iaco^a, D.E. Myers^b, D. Posa^{a,c,*}

^a*Facoltà di Economia, Dipartimento di Scienze Economiche e Matematico-Statistiche, Via per Monteroni, Ecotekne, 73100 Lecce, Italy*

^b*Dept of Mathematics, University of Arizona, 85721 Tucson AZ, USA*

^c*IRMA—CNR, Via Amendola 122/I 70126, Bari, Italy*

Received 1 April 2001; received in revised form 1 January 2002

Abstract

A space–time functional form for some contaminants is obtained and used for estimating total air pollution (TAP) in the district of Milan, Italy, during selected high-risk days of 1999. This functional form is determined through a space–time product–sum variogram model for TAP measurements and the dual form of kriging, i.e., radial basis functions. Data for nitric oxide (NO), nitrogen dioxide (NO₂) and carbon monoxide (CO) collected in Milan district, Italy are used to generate a combined indicator of traffic pollution, called TAP. In a previous study the weightings were obtained by multiple principal component analyses of the daily concentration levels. It was found that the first component explains approximately 70% of the total variance for each day and this component is treated as samples defined over space and time. A systematic pattern, which follows the corridor along which survey stations, characterized by heavy traffic are located, has been observed for TAP throughout Milan district, for all days considered. Note that the pollution data set is just an illustration for the new statistical method proposed. © 2002 Elsevier Science B.V. All rights reserved.

Keywords: Air pollution; Product–sum model; Radial basis functions; Space–time correlation models; Principal component analysis

* Corresponding author. Facoltà di Economia, Dipartimento di Scienze Economiche e Matematico-Statistiche, Via per Monteroni, Ecotekne, 73100 Lecce, Italy. Fax: +39-832-320-820.

E-mail addresses: sdeiac@tiscalinet.it (S. De Iaco), myers@math.arizona.edu (D.E. Myers), posa@economia.unile.it (D. Posa).

URLs: <http://www.u.arizona.edu/donaldm/>, <http://www.donatoposa.it>

1. Introduction

There are two ways of viewing the interpolation problem. In one case interpolation might be thought of as simply generating a contour map of the variable or variables of interest. Even from this perspective there is an advantage in generating a single measurement of pollution, i.e., a single map. However, the second perspective is that of generating an interpolating function which would then be amenable to further analysis as suggested by Myers (2001). The dual form of kriging estimator together with the space–time variogram model provides such an interpolating function and it has been used to generate an analytical form of the function for a synthetic measurement of pollution in order to describe its behavior over particular regions and risk days which were selected in a suitable way.

In a previous paper (De Iaco et al., 2001a) principal component analysis (PCA) was applied to an air pollution data set from Milan district, Italy, involving three contaminants (NO, NO₂ and CO) and the first component was considered as a measure of total air pollution (TAP), mainly caused by heavy traffic, in lieu of the separate contaminant concentrations. This component was treated as a sample from an unobserved variate defined over space and time and a space–time variogram was fitted to this new variate using the generalized product–sum model (De Iaco et al., 2001b), which has been used in the dual form of kriging to generate an interpolating function of TAP.

As outlined in Section 3, this last model is more general than a linear model, the product model and a product–sum model; moreover, it is not integrable, hence it cannot be obtained from the Cressie–Huang representation and it is flexible for estimating and modeling spatio-temporal correlation structures.

The PCA results can be used in several ways to produce a better picture of the air pollution levels both in space and time. One of the purposes of the following analysis is to find simple underlying components and to attribute physical meaning to them. Knowing the possible sources, their individual emissions would allow a comparison to determine if pollution is flowing into or out of a region. The comparison might also be used to determine if there are unidentified sources.

For example, in this study, six risk days have been selected and the interpolating function has been used to produce the corresponding maps of TAP in Milan district. A systematic pattern for TAP has been observed throughout Milan district, for all days considered: this pattern follows the corridor along which survey stations, characterized by heavy traffic, are located. Moreover, a second, less significant, pattern has been observed and it involves survey stations characterized by high-density population.

It is important to point out that the pollution data set from Milan district is just here an illustration for the new statistical method proposed.

2. Techniques for analyzing multivariate space–time data

Contaminants involved in air pollution are usually classified into two main groups: those emitted by vehicles (or resulting from chemical reactions involving emissions from vehicles) and contaminants emitted from industrial sources (and their by-products).

However, some contaminants may arise from either of these two general sources and monitoring equipment does not easily distinguish between the possible sources. The problem is complicated by both economic and physical constraints; each additional monitoring station represents a proportional increase in cost where as once established the station may easily collect data for multiple contaminants and may also collect data for a large number of time points; it may also not be easy or even possible to site monitoring stations in the most desirable locations.

Anyway, apart from sampling problems, a viable treatment of air pollution data should (a) consider multiple contaminants, (b) account for or incorporate the inter-variable correlation between contaminants, (c) account for or incorporate spatial correlation for each contaminant separately, (d) account for or incorporate temporal dependence for each contaminant.

In a spatio-temporal multivariate context, co-kriging would provide an appropriate tool for incorporating the spatio-temporal correlation of each contaminant as well as the inter-variable correlation. However, this requires solving two problems, adequately fitting valid spatio-temporal variograms or covariances and also adequately fitting valid spatio-temporal cross-variograms or cross-covariances. The problem can be simplified somewhat by generating a single measure of TAP. The simplest single measure would be a linear combination, then the problem is how to choose the weights in the linear combination. The weighting scheme should reflect the inter-variable correlation which may be time-dependent. Replacing the vector of contaminant values, at a given location and time, by a weighted linear combination is not quite optimal as shown in Myers (1983) but it has the advantage of only requiring the modeling of a single spatio-temporal variogram. An appropriate weighted linear combination might be more useful for detecting and identifying anomalous locations and/or dates than attempting to do this for each contaminant and possibly having conflicting indicators.

PCA is a widely used technique for identifying and removing the cross-correlation in multivariate data. Its application to climatic data is well documented in Preisendorfer (1988) with an emphasis on the use of empirical orthogonal functions. Several authors have considered the extension to data exhibiting spatial as well as temporal correlation, for example multivariate spatial and temporal correlation (Wackernagel, 1995). Statheropoulos et al. (1998) applied PCA to 5 years data concerning air pollutants and meteorological variables taken at one station (multivariate temporal analysis). These approaches usually define a vector of time or spatial-dependent second-order stationary random functions, whose components are related to different variables, respectively, at one station or time-point (Wackernagel, 1998).

PCA has been used previously in connection with kriging and cokriging in a slightly different but somewhat similar way. Coal has at least three important characteristics: sulfur content, ash and BTU content. Each of these affects the value of an amount of coal, a simple measure of value might then be a linear combination of the three characteristics. While in this case one might use exogenous information to determine the weighting scheme, there is still the question of whether to spatially analyse the three characteristics first and form a linear combination, or to analyse the simple measure of value. The former approach requires modeling both variograms and cross-variograms. The weighting scheme is then applied to the interpolated characteristics. Alternatively as

suggested above, interpolation of the linear combination would only require modeling of one variogram. Davis and Greenes (1983) used a slightly different approach: PCA was used to generate “new” characteristics, i.e., linear combinations of the original ones. These data were treated as samples from random functions representing the “new” variables and hence the data were used to model variograms for the “new” variables. They then verified that the sample cross-variograms justified the assumption that the “new” variables were spatially not cross-correlated. In that case, co-kriging the three “new” variates reduces to separate kriging of the three.

As mentioned above, in this paper PCA has been used to determine a weighting scheme for a linear combination of the contaminants considered, and the first component has been considered as a measure of TAP, however, the question of modelling it remains an open problem.

3. The data set

As it was pointed out (De Cesare et al., 1997), air pollution in Milan district, may be attributed to different factors: emissions from motor vehicles, manufacturing and heating systems during winter.

Although several pollutants are provided by the monitoring system in Milan district, contaminants, mainly caused by heavy traffic, whose measuring devices are located close to the main urban center streets or motorways, are chosen. For this reason, other pollutants, even critical for the public health, have been left out; such as ozone (O_3) which is caused by complex photochemical processes. In particular, the air pollution data set involves three contaminants, NO, NO_2 and CO, available at 30 locations, taken hourly during the whole 1999 and converted to daily averages; then, these values have been standardized. The air pollution monitoring network for NO, NO_2 and CO is shown in Fig. 1, where the following classification of the monitoring stations according to the Premier’s Decree in 1991 is pointed out:

- stations characterized by high-density population (solid squares);
- stations characterized by heavy traffic (solid circles).

It is important to point out that, up to the present, this work is not supported by a grant or a joint work with pollution engineers. Indeed, the environmental protection system is only in charge of collecting the concentration values of various pollutants and atmospheric variables according to the national law and bringing under control the most dangerous pollutants without analyzing in detail of the fundamental issues concerning environmental protection.

In a previous paper (De Iaco et al., 2001a) PCA was applied to each of the 365 standardized data sets (3 contaminants and 30 stations) and it was shown that the first component explains approximately 70% of the total variance for each day although this dominance is reduced in summer. While the mixing of contaminants on any 1 day is relatively fixed, this mixing can easily change from one to another due to the day of the week, the season of the year, factory scheduling, changes in traffic densities.

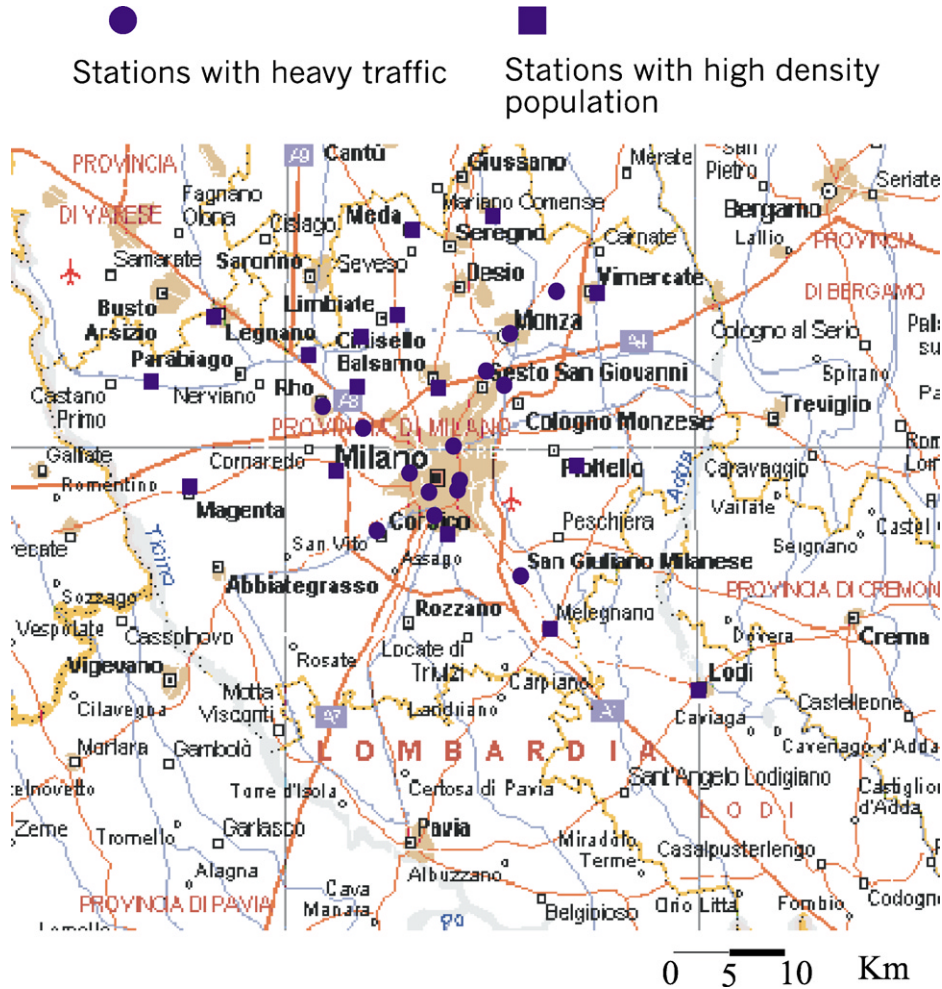


Fig. 1. Posting map of 30 survey stations in Milan district and their classification.

For the first component, all the linear combinations for which the eigenvectors had the sign pattern $(+, +, +)$ for NO , NO_2 and CO , were considered. Since the loadings, selected in such a way, were all positive and almost equal, the above linear combinations has been reasonably interpreted as a measure of TAP generated by NO , NO_2 and CO and used in this study.

Indeed, if the loadings are almost of the same magnitude and all positive, the corresponding principal component variate is called size factor, in the sense that it is considered as an index that best summarizes the data (Dunteman, 1989).

Fig. 2 shows the histogram of TAP values. In order to select the days of 1999 for which pollution concentrations are both critical and more spread out, the following

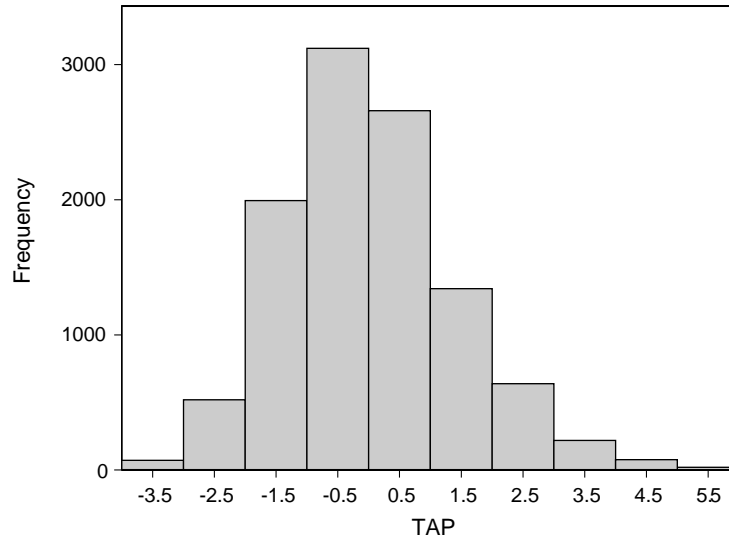


Fig. 2. Histogram of TAP values.

procedure has been adopted:

- the 90th and the 95th percentiles of TAP values have been considered;
- the days for which at least five stations present values of TAP greater than the 90th percentile have been selected;
- the days for which at least three stations present values of TAP greater than the 95th percentile have been chosen;
- the days resulting from the intersection have been selected.

In Fig. 3 the shape of the posting symbol varies according to the frequency of values for TAP greater than the 90th percentile. Note that the distinction between the two types of the stations has been preserved as in Fig. 1, that is empty symbols are used for high density population stations and solid symbols for heavy traffic stations.

4. Space–time correlation models

Besides some classes of spatio-temporal covariance models that have appeared in the literature, the product–sum covariance model and the generalized product–sum covariance model, which has been used in this paper, are briefly presented in this section.

Consider a space–time second-order stationary random field:

$$Z = \{Z(\mathbf{s}, t), (\mathbf{s}, t) \in D \times T\}, \quad (1)$$

where $D \subset \mathfrak{R}^d$ and $T \subset \mathfrak{R}_+$, with covariance:

$$C_{st}(\mathbf{h}) = Cov(Z(\mathbf{s} + \mathbf{h}_s, t + h_t), Z(\mathbf{s}, t)), \quad (2)$$

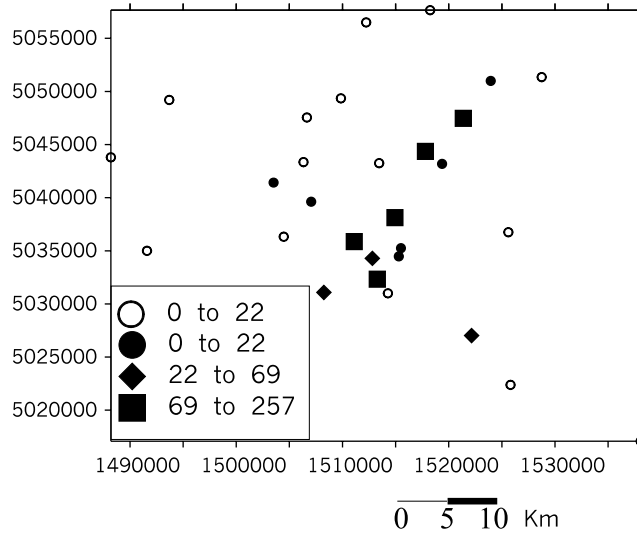


Fig. 3. Posting map of the monitoring stations where TAP values were greater than the 90th percentile.

and variogram:

$$2\gamma_{st}(\mathbf{h}) = \text{Var}(Z(\mathbf{s} + \mathbf{h}_s, t + h_t) - Z(\mathbf{s}, t)), \tag{3}$$

where $\mathbf{h} = (\mathbf{h}_s, h_t)$, $(\mathbf{s}, \mathbf{s} + \mathbf{h}_s) \in D^2$ and $(t, t + h_t) \in T^2$.

(1) For the *metric model* (Dimitrakopoulos and Luo, 1994), it is assumed that:

$$C_{st}(\mathbf{h}_s, h_t) = C(a^2|\mathbf{h}_s|^2 + b^2h_t^2), \tag{4}$$

where the coefficients $a, b \in \mathfrak{R}$. Note that in (4) the same type of model is assumed for the spatial and temporal covariances, with possible changes in the range.

(2) In the *product model* (De Cesare et al., 1997), the spatio-temporal covariance is:

$$C_{st}(\mathbf{h}_s, h_t) = C_s(\mathbf{h}_s)C_t(h_t), \tag{5}$$

where the spatial dependence is separated by the temporal one. In (5) C_s is a positive-definite function in \mathfrak{R}^d and C_t is a positive-definite function in \mathfrak{R} ; admissible spatial covariance models and admissible temporal covariance models are readily available (Cressie, 1993), hence they can be combined in product form to give spatio-temporal covariance models. However, the class (5) is severely limited, since for any pair of spatial locations the cross-covariance function of the two time series always has the same shape. In fact, for any two fixed spatial lags \mathbf{h}_1 and \mathbf{h}_2 , it results that:

$$C_{st}(\mathbf{h}_1, h_t) \propto C_{st}(\mathbf{h}_2, h_t).$$

A similar result holds for any pair of time points and the cross-covariance function of the two spatial processes.

(3) *The linear model.* Another type of separability involves adding spatial and temporal covariances (Rouhani and Hall, 1989), that is:

$$C_{st}(\mathbf{h}_s, h_t) = C_s(\mathbf{h}_s) + C_t(h_t). \quad (6)$$

For this model, covariance matrices of certain configurations of spatio-temporal data are singular (Myers and Journel, 1990): in this case, the covariance function is only positive semidefinite and it is unsatisfactory for optimal prediction.

(4) *The nonseparable model.* A new approach that allows us to obtain classes of non-separable, spatio-temporal stationary covariance functions has been derived by Cressie and Huang (1999). The authors assume that:

$$C_{st}(\mathbf{h}_s, h_t) = \int e^{i\mathbf{h}_s^T \omega} \rho(\omega, h_t) k(\omega) d\omega, \quad (7)$$

where the following two conditions are satisfied:

- for each $\omega \in \mathfrak{R}^d$, $\rho(\omega, \cdot)$ is a continuous autocorrelation function and $k(\omega) > 0$;
- the positive function $k(\omega)$ satisfies:

$$\int k(\omega) d\omega < \infty.$$

(5) The *product–sum covariance model* can be obtained in the following way:

$$C_{st}(\mathbf{h}_s, h_t) = k_1 C_s(\mathbf{h}_s) C_t(h_t) + k_2 C_s(\mathbf{h}_s) + k_3 C_t(h_t), \quad (8)$$

or equivalently, in terms of the semivariogram function:

$$\gamma_{st}(\mathbf{h}_s, h_t) = [k_2 + k_1 C_t(0)] \gamma_s(\mathbf{h}_s) + [k_3 + k_1 C_s(\mathbf{0})] \gamma_t(h_t) - k_1 \gamma_s(\mathbf{h}_s) \gamma_t(h_t), \quad (9)$$

where C_s and C_t are covariance functions, γ_s and γ_t are the corresponding semivariogram functions and $k_1 > 0$, $k_2 \geq 0$, $k_3 \geq 0$ to ensure admissibility. Note that $C_{st}(\mathbf{0}, 0)$ is the sill of γ_{st} (“global” sill), $C_s(\mathbf{0})$ is the sill of γ_s and $C_t(0)$ is the sill of γ_t ($C_s(\mathbf{0})$ and $C_t(0)$ are named “partial” sills).

4.1. The generalized product–sum model

A generalization of the product–sum covariance model introduced by De Cesare et al. (2001b) is given by the generalized product–sum model (De Iaco et al., 2001b):

$$\gamma_{st}(\mathbf{h}_s, h_t) = \gamma_{st}(\mathbf{h}_s, 0) + \gamma_{st}(\mathbf{0}, h_t) - k \gamma_{st}(\mathbf{h}_s, 0) \gamma_{st}(\mathbf{0}, h_t), \quad (10)$$

where $\gamma_{st}(\mathbf{h}_s, 0)$ and $\gamma_{st}(\mathbf{0}, h_t)$ are valid spatial and temporal bounded variogram functions and

$$k = \frac{(\text{sill} \gamma_{st}(\mathbf{h}_s, 0) + \text{sill} \gamma_{st}(\mathbf{0}, h_t) - \text{sill} \gamma_{st}(\mathbf{h}_s, h_t))}{(\text{sill} \gamma_{st}(\mathbf{h}_s, 0) \text{sill} \gamma_{st}(\mathbf{0}, h_t))}. \quad (11)$$

Theoretical results are given in De Iaco et al. (2001b) and a modification of the GSLIB software (Deutsch and Journel, 1997) to apply the product–sum model is given in De Cesare et al. (2002). An application of the product–sum model and some theoretical results are given in De Cesare et al. (2001a, b).

In modelling the separate spatial and temporal variograms, the sills which are chosen allow specifying the sufficient condition of admissibility for $\gamma_{st}(\mathbf{h}_s, h_t)$ is satisfied, namely:

$$0 < k \leq 1/\max\{\text{sill}(\gamma_{st}(\mathbf{h}_s, 0)), \text{sill}(\gamma_{st}(\mathbf{0}, h_t))\}. \quad (12)$$

Note that k is selected in such a way to ensure that the global sill is fitted.

4.2. Some general comments

A brief comparative study among the classes of models previously described has been made in this section. Particularly:

- if the autocorrelation function ρ in (7) is purely a function of h_t , then the product covariance model is obtained;
- the product model and the linear model are easily obtained by the product–sum covariance model setting, respectively, $k_2 = k_3 = 0$ and $k_1 = 0$;
- the product–sum covariance model and the generalized product–sum covariance model are non-separable and, in general, are non-integrable, hence they cannot be obtained from the Cressie–Huang representation. Moreover, the product–sum covariance model and the generalized product–sum covariance model do not require the use of a metric in space–time;
- the product–sum covariance model and the generalized product–sum covariance model are more flexible than the non-separable covariance model for estimating and modelling spatio-temporal correlation structures.

4.3. Space–time variogram modelling

The space–time analysis has been performed by using the data for TAP at 30 monitoring stations for all 365 days of 1999. TAP measurements are considered as a realization of a space–time second-order stationary random field:

$$Z = \{Z(\mathbf{s}, t), (\mathbf{s}, t) \in D \times T\}, \quad (13)$$

where $D \subset \mathfrak{R}^2$ and $T \subset \mathfrak{R}_+$, with variogram:

$$2\gamma_{st}(\mathbf{h}) = \text{Var}(Z(\mathbf{s} + \mathbf{h}_s, t + h_t) - Z(\mathbf{s}, t)), \quad (14)$$

where $\mathbf{h} = (\mathbf{h}_s, h_t)$, $(\mathbf{s}, \mathbf{s} + \mathbf{h}_s) \in D^2$ and $(t, t + h_t) \in T^2$.

The sample spatial and temporal variograms for TAP and their models are shown in Fig. 4(a) and (b). Note that the temporal variogram highlights the weekly seasonality presented by the data.

Analytical expressions for the fitted models are given below:

$$\gamma_{st}(\mathbf{h}_s, 0) = 2(1 - \exp(-\mathbf{h}_s/2000)), \quad (15)$$

$$\gamma_{st}(\mathbf{0}, h_t) = 0.64(1 - \exp(-h_t/1.6)) + 0.26(1 - \cos(h_t 2\pi/7)). \quad (16)$$

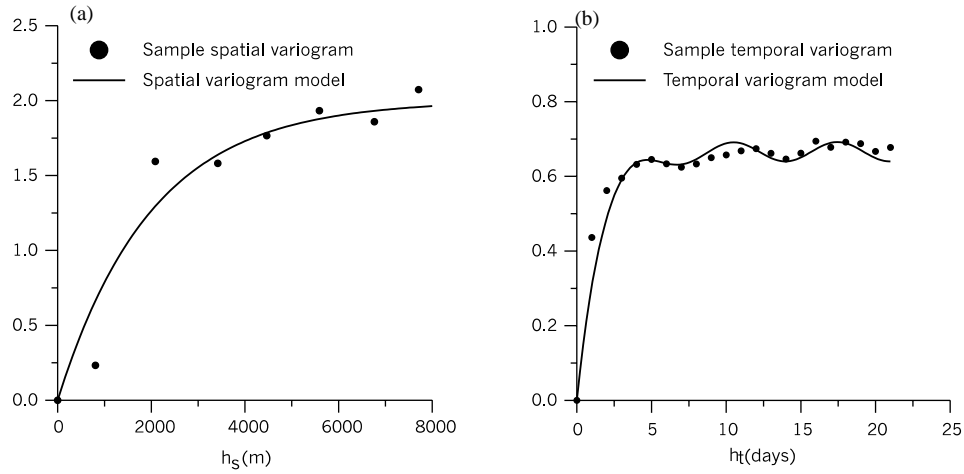


Fig. 4. Sample spatial and temporal variograms and their models.

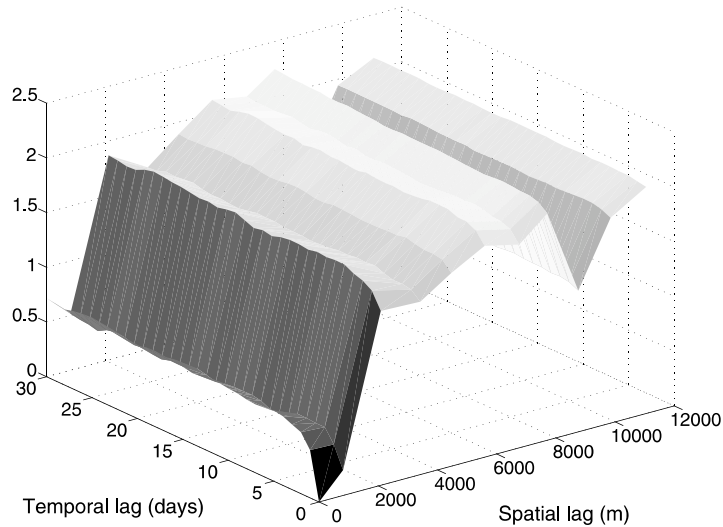


Fig. 5. Sample space–time variogram surface.

In order to compute (11) and generate the model (10) which can then be used for prediction in space and time, the sill value $C_{st}(\mathbf{0}, 0)$ of $\gamma_{st}(\mathbf{h}_s, h_t)$ (called “global” sill in the literature) has been estimated graphically by plotting the spatio-temporal variogram surface (Fig. 5).

The “global” sill value for TAP is 2.2 and the resulting space–time admissible model is:

$$\gamma_{st}(\mathbf{h}_s, h_t) = \gamma_{st}(\mathbf{h}_s, 0) + \gamma_{st}(\mathbf{0}, h_t) - 0.39[\gamma_{st}(\mathbf{h}_s, 0)\gamma_{st}(\mathbf{0}, h_t)]. \quad (17)$$

As pointed out in Section 2, 6 days (the 6th of March, the 9th of April, the 31st of May, the 6th of August, the 8th of October and the 5th of December), which have met the criteria, have been retained for the following analysis. Goodness of the fitted product–sum model (17) has been evaluated for those days at the monitoring stations through cross-validation. For each risk day, the space–time neighborhood, used to estimate at the monitoring stations, is the following:

- (1) 3 days before and 3 days after the risk day;
- (2) spatial range of the space–time model.

Fig. 6 shows the scatter plots of true values vs. estimates together with the correlation coefficients.

5. Functional form of interpolators

Kriging written in the dual form is the same as what is known in the numerical analysis literature as radial basis functions (RBF), the thin plate spline (TPS) is a special case of both. The functional form for the interpolator is the same for dual kriging and RBF (Myers, 1992). The TPS corresponds to a specific generalized covariance, whereas the kriging estimator or the radial basis function interpolator only requires the use of a kernel with appropriate positive definiteness properties. This allows adapting the kernel function to a particular data set. The extension of space–time kriging to RBF's is given in Myers et al. (2002) and it is briefly reviewed herein. Let $Z(\mathbf{s}, t)$ denote the function representing the concentration of the contaminant of interest at space location \mathbf{s} and time t , then the dual kriging/RBF interpolator of this unknown function is given by:

$$\hat{Z}(\mathbf{s}, t) = \sum_{i=1}^n b_i g(\mathbf{s} - \mathbf{s}_i, t - t_i) + \sum_{k=0}^p a_k f_k(\mathbf{s}, t), \quad (18)$$

where

$$(\mathbf{s}_i, t_i), \quad i = 1, \dots, n$$

are the data locations and g is the spatio-temporal variogram (10). The unknown coefficients in this interpolating function are obtained as the solution of a system of linear equations. The $f_k(\mathbf{s}, t)$, $k = 0, \dots, p$ are linearly independent functions, usually monomials in the coordinates (\mathbf{s}, t) . Although it would be unlikely that the f_k 's would be periodic in the position coordinates, it is likely that sine, cosine terms in the time coordinate could be included. These terms correspond to the mean function of the random function $Z(\mathbf{s}, t)$ or to the null space of the operator in the case of RBF's. As an alternative to incorporating non-constant f_k 's, one may fit the data to a trend surface (polynomial functions in the space coordinates and periodic functions in the time coordinate), then the residual data are used for the analysis, later the fitted trend surface is added back.

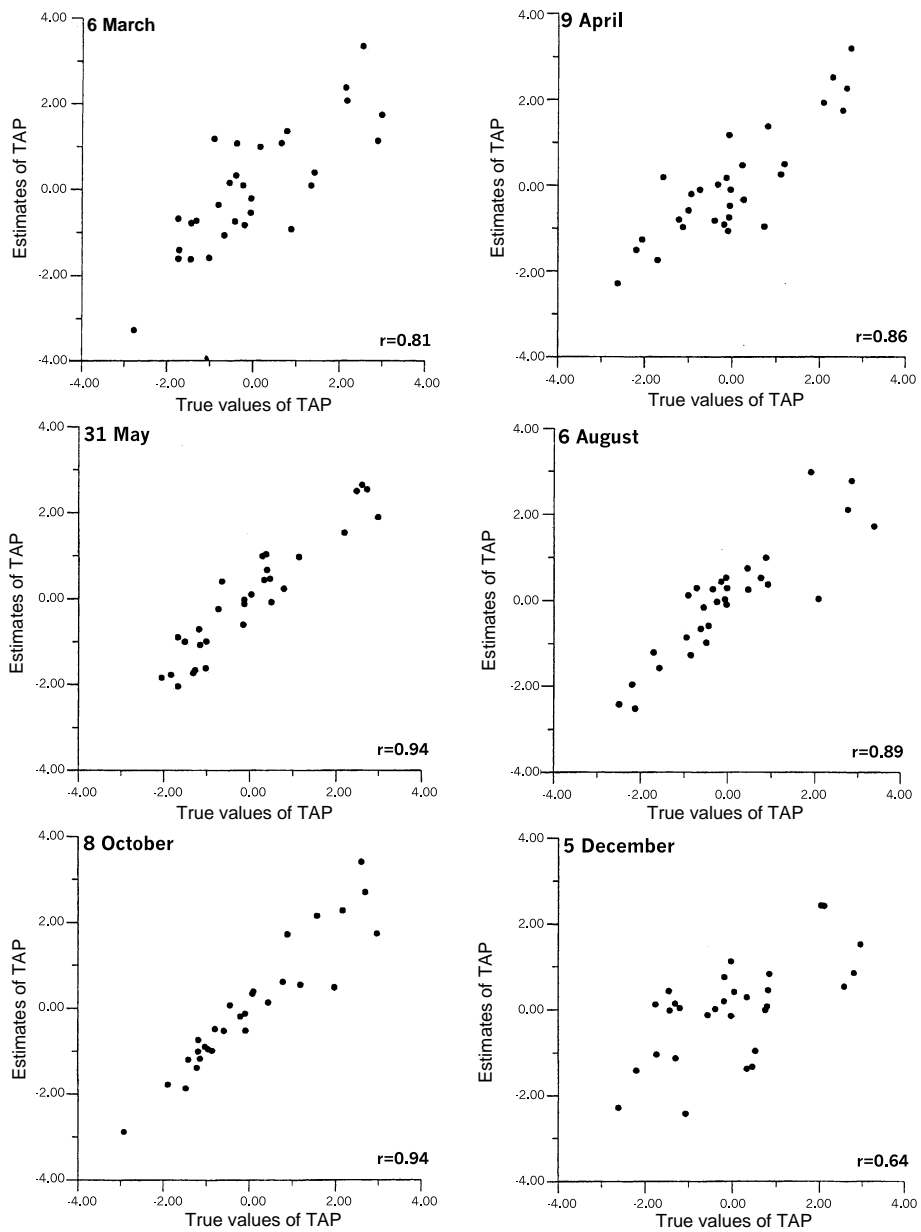


Fig. 6. Scatter plot of the true values vs. estimated values.

5.1. Space–time RBF for TAP

To illustrate the use of the interpolating function approach to characterizing a contaminant plume, the dual form of kriging (18), where g is the space–time variogram given in (17), has been used to estimate TAP throughout Milan district for the six high risk days previously identified for 1999. The data do not exhibit any significant spatial non-stationarity and the temporal seasonal component is included in the variogram as described in Section 3. Thus in this application $f_0(\mathbf{s}, t) = 1$ and $f_k(\mathbf{s}, t) = 0$, $k = 1, \dots, p$.

Particularly, let t_j , $j = 65, 99, 151, 218, 281, 339$ be the risk days, the coefficients b_j for the interpolator associated to each risk day t_j , have been estimated taking into account all the data points belonging to the following set:

$$\{(\mathbf{s}_i, t_{j+k}), i = 1, \dots, 30, k = -3, -2, -1, 1, 2, 3\}.$$

Figs. 7 and 8 show the contour maps for these high-risk days.

5.2. Numerical problems

In its usual form, the coefficients in the kriging estimator can be obtained “locally”, i.e., one need not use the entire data-set to solve the system of equations but rather a moving search window is used. In the dual form, this approach cannot be used in such a simple form. The difficulty is greatly exaggerated in the space–time context because while the number of monitoring stations may be small, data will be collected at a large number of time points thus the entire data set is large. This problem has been addressed in Schaback and Wendland (2000), Faul and Powell (2000), Auñón and Gómez-Hernández (2000).

6. Results

As it was pointed out in Section 2, the risk days have been selected using two combined criteria. Six days (the 6th of March, the 9th of April, the 31st of May, the 6th of August, the 8th of October and the 5th of December) which have met both criteria have been retained.

From Figs. 7 and 8, note that a systematic pattern for TAP is observed, for all days considered: this pattern follows the corridor along which survey stations, characterized by heavy traffic, are located. Particularly, the monitoring stations, which most frequently have high values for TAP, are primarily located in the city of Milan and the north eastern part of the district. A second, less significant, pattern is also observed for some days and it involves survey stations characterized by high-density population, as it was pointed out in Fig. 1: the corresponding monitoring stations are located in the north western and south eastern part of the district.

Note that only one risk day (the 6th of August) has been detected in summer time, hence total air pollution should present lower relative values during this season, with respect to the rest of the year. This is because either the atmospheric conditions help

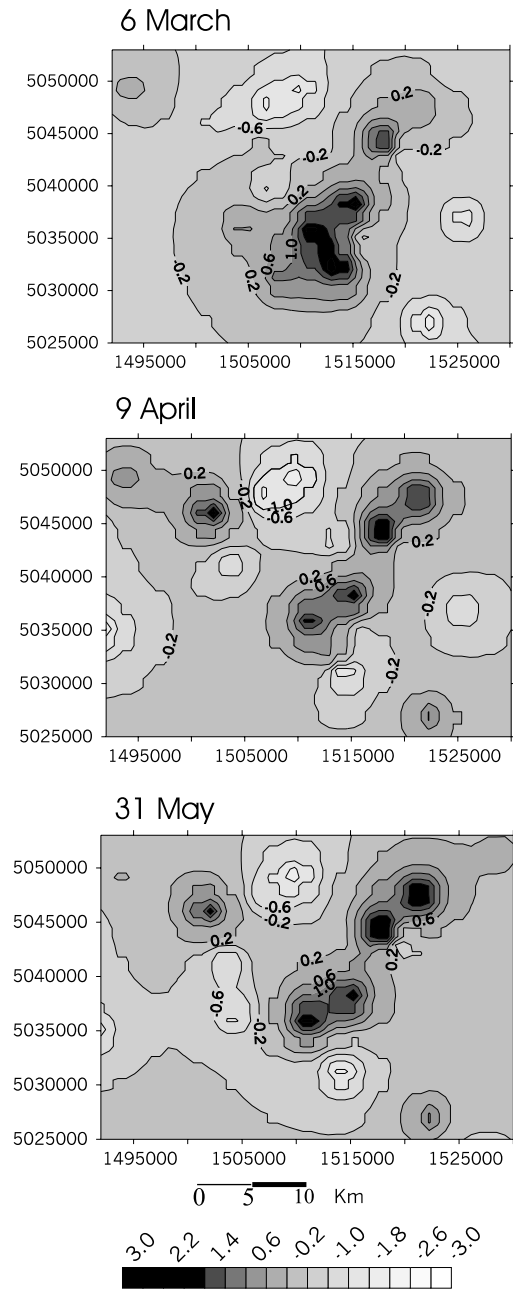


Fig. 7. Contour maps of TAP for the risk days: 6 April, 9 March and 31 May.

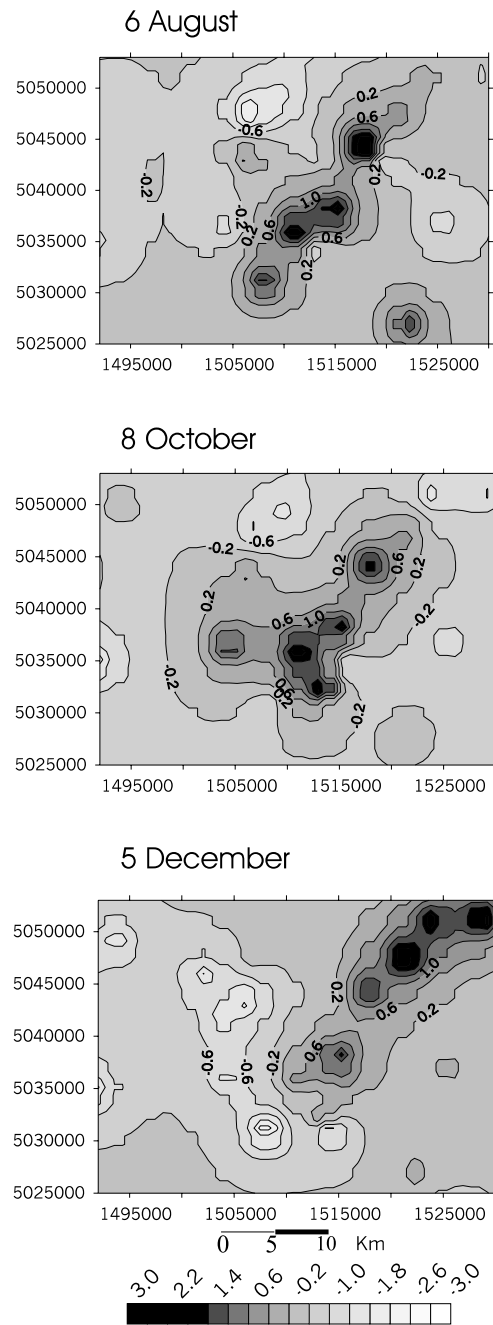


Fig. 8. Contour maps of TAP for the risk days: 6 August, 8 October and 5 December.

the dispersion of pollutants or lower traffic characterizes the monitoring stations as defined in Section 2.

7. Summary and conclusions

In this paper a new statistical method for conducting spatio-temporal analysis is proposed. Particularly, a space–time functional form is considered for estimating TAP in Milan district, Italy, using data of different atmospheric pollutants, observed irregularly over space and regularly over time. Then, air pollution patterns in Milan district, during 1999 have been analyzed using this measurements of TAP, constructed as a linear combination of the daily averages of NO, NO₂ and CO, whose weights were determined by the use of PCA. TAP measurements have been considered as realization of a random function defined in space–time and they have been modeled by using a generalized product-sum model. The monitoring stations, which most frequently have high values for TAP, are primarily located in heavy traffic area, that is in the city of Milan and the north eastern part of the district.

In the appendix some advantages of using the RBF approach are outlined.

Appendix A. Advantages of using a RBF

As noted above, $Z(\mathbf{s}, t)$ is assumed to represent the concentration of a contaminant at the space–time point $(\mathbf{s}, t) \in \mathcal{R}^d \times T$, then the “plume” is the set of points where $Z(\mathbf{s}, t) > 0$. More precisely, let

$$\mathbf{P}(t) = \{\mathbf{s} \in \mathcal{R}^d \mid Z(\mathbf{s}, t) > 0\}, \quad (\text{A.1})$$

then $\mathbf{P}(t)$ is a set of points in space which can change with time. Properties of the plume can be described in terms of the (unknown) function $Z(\mathbf{s}, t)$ and these properties/characteristics can be estimated by $\hat{Z}(\mathbf{s}, t)$. Considering the indicator function of $Z(\mathbf{s}, t)$:

$$I_Z(\mathbf{s}, t; z) = \begin{cases} 1 & Z(\mathbf{s}, t) \leq z, \\ 0 & Z(\mathbf{s}, t) > z, \end{cases} \quad (\text{A.2})$$

the volume of the plume at time t is given by:

$$\mathbf{V}(t) = \int_{\mathcal{R}^d} [1 - I_Z(\mathbf{s}, t; 0)] \, d\mathbf{s}. \quad (\text{A.3})$$

If the plume is bounded in space then the boundedness of the integrand is sufficient to ensure that the integral exists. Because instrumentation and/or analytical procedures will nearly always have a detection limit that is greater than zero, when using data to estimate the plume volume it will be more appropriate to use a slightly positive cut-off value in lieu of zero. The rate of change of the volume of the plume would then be given by the time derivative:

$$\frac{d}{dt} \mathbf{V}(t). \quad (\text{A.4})$$

While it might not be reasonable to expect the indicator function to be smooth as a function of the space coordinates, it is more reasonable to expect it to be smooth, i.e., differentiable with respect to the time variable.

The total amount of contaminant in the plume, at time t is given by:

$$\mathbf{T}(t) = \int_{\mathbf{P}(t)} Z(\mathbf{s}, t) \, ds. \quad (\text{A.5})$$

The total contaminant concentration in the plume may be of interest because in some instances it will be possible to determine the total pollution independently of estimating this integral and as such would allow a check on the modeling of the plume function. Of course the average concentration of the contaminant in the plume would be given by:

$$\overline{\mathbf{T}(t)/\mathbf{V}(t)},$$

and the rate of change of the average concentration is given by:

$$\frac{d}{dt} [\overline{\mathbf{T}(t)/\mathbf{V}(t)}]. \quad (\text{A.6})$$

However, in some instances it might be useful to compute the average of a fixed spatial area rather than over the entire plume. Of course the rate of change of the total concentration would be given by:

$$\frac{d}{dt} \mathbf{T}(t).$$

If the function $Z(\mathbf{s}, t)$ is sufficiently smooth with respect to time, then

$$\mathbf{R}(\mathbf{s}) = \frac{d}{dt} Z(\mathbf{s}, t) \quad (\text{A.7})$$

would be the local rate of change of concentration. The set of points, in space, where this derivative is zero would represent a stagnant area.

References

- Auñón, J., Gómez-Hernández, J.J., 2000. Dual kriging with local neighborhoods: application to the representation of surfaces. *Math. Geol.* 32 (1), 69–86.
- Cressie, N., Huang, H., 1999. Classes of nonseparable, spatio-temporal stationary covariance functions. *JASA* 94, 1330–1340.
- Davis, B., Greenes, A., 1983. Estimation using distributed multivariate data: an example with coal quality. *Math. Geol.* 15 (2), 287–300.
- De Cesare, L., Myers, D.E., Posa, D., 1997. Spatial temporal modeling of SO₂ in the Milan district. In: Baafi, E.Y., Schofield, N.A. (Eds.), *Geostatistics Wollongong '96*, Vol. 2. Kluwer Academic Publishers, Dordrecht, pp. 1031–1042.
- De Cesare, L., Myers, D.E., Posa, D., 2002. FORTRAN programs for space–time modeling. *Comput. Geosci.* 28, 205–212.
- De Cesare, L., Myers, D.E., Posa, D., 2001a. Product–sum covariance for space–time modeling: an environmental application. *Environmetrics* 12, 11–23.
- De Cesare, L., Myers, D.E., Posa, D., 2001b. Estimating and modelling space–time correlation structures. *Statist. Probab. Lett.* 51 (1), 9–14.

- De Iaco, S., Myers, D.E., Posa, D., 2001a. Total air pollution and space–time modelling. In: Monestiez, P., Allard, D., Froidevaux, R. (Eds.), *GeoEnv III—Geostatistics for Environmental Applications*. Kluwer Academic Publishers, Dordrecht, pp. 45–56.
- De Iaco, S., Myers, D.E., Posa, D., 2001b. Space–time analysis using a general product–sum model. *Statist. Probab. Lett.* 52 (1), 21–28.
- Deutsch, C.V., Journel, A.G., 1997. *GSLIB: Geostatistical Software Library and User’s Guide*. Oxford University Press, New York.
- Dimitrakopoulos, R., Luo, X., 1994. *Spatiotemporal Modelling: Covariances and Ordinary Kriging Systems. Geostatistics for the next century*. Kluwer Academic Publishers, Dordrecht, 88–93.
- Dunteman, G.H., 1989. *Principal Component Analysis*. Sage Publications Inc., Newbury Park.
- Faul, A.C., Powell, M.J.D., 2000. Krylov Subspace Methods for Radial Basis Function Interpolation. *Chapman & Hall/CRC Res. Notes Math* 420, 115–141.
- Myers, D.E., 1983. Estimation of linear combinations and cokriging. *Math. Geol.* 15, 633–637.
- Myers, D.E., 1992. Kriging, cokriging, radial basis functions and the role of positive definiteness. *Comput. Math. Appl.* 24 (12), 139–148.
- Myers, D.E., 2001. Space–time correlation models and contaminant plumes. *Environmetrics*, to appear (papers from the Fourth International Conference on Environmetrics and Chemometrics, Las Vegas, NV, September 2000).
- Myers, D.E., De Iaco, S., Posa, D., De Cesare, L., 2002. Space–time radial basis functions. *Comput. Math. Appl.* 43, 539–549.
- Myers, D.E., Journel, A.G., 1990. Variograms with zonal anisotropies and non-invertible kriging systems. *Math. Geol.* 22, 779–785.
- Preisendorfer, R.W., 1988. *Principal Component Analysis in Meteorology and Oceanography*. Elsevier, Amsterdam, 425pp.
- Rouhani, S., Hall, T.J., 1989. Space–time Kriging of Groundwater Data. *Geostatistics*. Kluwer Academic Publishers, Dordrecht, Vol. 2, pp. 639–651.
- Schaback, R., Wendland, H., 2000. Adaptive greedy techniques for approximate solution of large RDF systems. *Numer. Algor.* 24, 239–254.
- Statheropoulos, M., Vassiliadis, N., Pappa, A., 1998. Principal component and canonical correlation analysis for examining air pollution and meteorological data. *Atmos. Environ.* 6, 1087–1095.
- Wackernagel, H., 1995. *Multivariate Geostatistics*. Springer, New York.
- Wackernagel, H., 1998. *Principal component analysis for autocorrelated data: a geostatistical perspective*. Technical report, Centre de Geostatistique, Ecole de Mines de Paris.